Direct Observation of Flatband Loop States Arising from Nontrivial Real-Space Topology

Jina Ma,[1,‡] Jun-Won Rhim,[2,3,‡] Liqin Tang,[1,4,*] Shiqi Xia,[1] Haiping Wang,[1] Xiuyan Zheng,[1] Shiqiang Xia,[1,5] Daohong Song,[1,4] Yi Hu,[1,4] Yigang Li,[1] Bohm-Jung Yang,[2,3,6] Daniel Leykam,[7] and Zhigang Chen[1,4,8,†]

[1]*The MOE Key Laboratory of Weak-Light Nonlinear Photonics, TEDA Applied Physics Institute and School of Physics, Nankai University, Tianjin 300457, China*

[2]*Department of Physics and Astronomy, Seoul National University, Seoul 08826, Korea*

[3]*Center for Correlated Electron Systems, Institute for Basic Science (IBS), Seoul 08826, Korea*

[4]*Collaborative Innovation Center of Extreme Optics, Shanxi University, Taiyuan, Shanxi 030006, People's Republic of China*

[5]*Engineering Lab for Optoelectronic Technology and Advanced Manufacturing, Henan Normal University, Xinxiang, 453007, China*

[6]*Center for Theoretical Physics (CTP), Seoul National University, Seoul 08826, Korea*

[7]*Center for Theoretical Physics of Complex Systems, Institute for Basic Science, Daejeon 34126, Republic of Korea*

[8]*Department of Physics and Astronomy, San Francisco State University, San Francisco, California 94132, USA*

(Received 1 November 2019; accepted 16 April 2020; published 4 May 2020)

Topological properties of lattices are typically revealed in momentum space using concepts such as the Chern number. Here, we study unconventional loop states, namely, the noncontractible loop states (NLSs) and robust boundary modes, mediated by nontrivial topology in real space. While such states play a key role in understanding fundamental physics of flatband systems, their experimental observation has been hampered because of the challenge in realizing desired boundary conditions. Using a laser-writing technique, we optically establish photonic kagome lattices with both an open boundary by properly truncating the lattice, and a periodic boundary by shaping the lattice into a Corbino geometry. We thereby demonstrate the robust boundary modes winding around the entire edge of the open lattice and, more directly, the NLSs winding in a closed loop akin to that in a torus. We prove that the NLSs due to real-space topology persist in ideal Corbino-shaped kagome lattices of arbitrary size. Our results could be of great importance for our understanding of the singular flatbands and the intriguing physics phenomenon applicable for strongly interacting systems.

DOI: 10.1103/PhysRevLett.124.183901

A flatband (FB) is a dispersion-free energy band where the group velocity vanishes at all momenta in the Brillouin zone and thus electrons are considered immobile or localized. FB systems have attracted considerable interest in many different branches of physics in past decades, partly because interaction effects in such systems are maximized by the zero kinetic energy. Much progress has been made in understanding fundamental phenomena associated with FB lattices, including Anderson localization, bosonic condensation, parity-time symmetry, fractional quantum Hall states, superconducting transitions, and superfluidity in topological FBs [1–11]. Indeed, engineered FB structures have now been realized in a variety of physical systems [12], ranging from photonic waveguide arrays [13–22] to synthetic atomic lattices [23,24], and from metamaterials [25] to cavity polaritons [26]. Recently, FB structures have also been experimentally accomplished in realistic materials forming electronic Lieb and kagome lattices [27,28].

The localized nature of the FB states is clearly characterized by the existence of the so-called compact localized states (CLSs), which are the exact FB eigenstates with nonzero amplitudes only in a few lattice sites inside a finite region, as demonstrated already in several photonic experiments [14–19]. An example with the kagome lattice (KL) is illustrated in Fig. 1(a), which has an FB touching a dispersive band in momentum space [Fig. 1(b)]. As discussed in condensed matter physics, although an electron can hop between lattice sites, these localized eigenstates do not spread out due to destructive interference. A linear combination of Bloch wave functions always exists which results in the CLSs in the FB systems [12,29,30]. In principle, there should be N linearly independent CLSs to span the whole FB, where N is the number of unit cells. If the Bloch wave function has a discontinuity in momentum space due to the singular band crossing, the maximum number of linearly independent CLSs is always less than N, and the missing states are the so-called noncontractible loop states (NLSs) that manifest the topological properties in real space as discussed in Refs. [29,30].

One can understand this intuitively as follows: First, as shown for the KL in Fig. 1(c), the NLSs extend unboundedly in an infinite lattice. With a torus geometry, equivalent to imposing a periodic boundary condition (BC), an NLS spans a closed loop across the torus along either toroidal or poloidal direction [see Fig. 1(d)] that defines the winding.

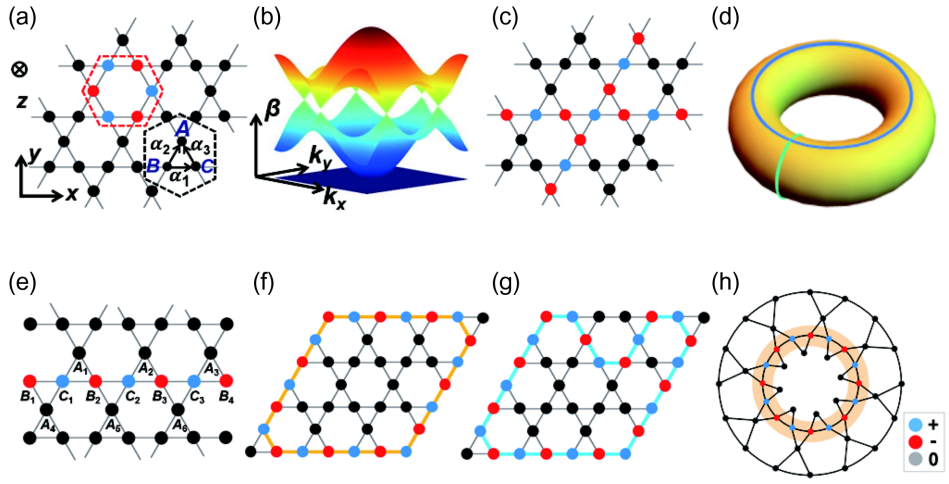

FIG. 1. (a) Schematic of a kagome lattice (KL), where the black dashed hexagon marks a unit cell with three sublattice sites labeled A, B, and C and a set of lattice vectors denoted as α_n ($n = 1, 2, 3$), and the red dashed hexagon represents a simplest CLS. (b) Band structure in the tight-binding approximation. (c) Illustration of two NLSs in an infinitely extended lattice. (d) A torus showing two NLSs mimicking an infinite lattice. (e) A KL terminated with zigzag-armchair edges in left and right sides, where the colored dots illustrate a line state. (f),(g) A lattice terminated with all flat-cutting edges, and orange (blue) loop illustrates the boundary mode RBM1 (RBM2). (h) A Corbino-shaped KL, where the orange loop illustrates an NLS. In all figures, black sites are of zero amplitude, while blue and red ones distinguish nonzero sites with opposite phase.

Second, the NLSs are robust against the addition of any CLS or local perturbation, because it cannot break an NLS but only warps its loop, and the resulting NLS is again an eigenstate. Third, in a finite system with open BCs, the NLSs are revealed by the robust boundary modes (RBMs), which span a closed contour along the boundary of the entire finite system. These RBMs can be considered as a direct consequence of cutting and folding the 3D torus into a 2D plane, manifesting the NLSs[30]. Both the NLSs and the RBMs characterize the Bloch wave function discontinuity of the singular FB, establishing the novel bulk-boundary correspondence. When they are present, the topological structure protects the band touching in a sense that they can only be removed by strong perturbations that also destroy the flatness of the energy band. Because of the localized characteristic and nontrivial winding of these FB states, the topological protection lies in real space rather than in momentum space [29,30].

Although these results have been predicated theoretically, direct observation of the NLSs has been a challenge because they are stable only under the periodic BC or on the torus geometry of the lattice model, while in real-world experiments the lattices are usually finite with open boundaries. In a recent effort to achieve this goal, line states were realized in a finite Lieb lattice with specially designed boundaries [22]. The line states look quite similar to the NLSs, but they can represent only an indirect and incomplete demonstration of the NLSs because the stability of those line states greatly depends on a specific boundary shape. Naively, we would expect the NLSs should also be observed in the widely studied KLs [31–37]. However, in a finite KL, it is even impossible to stabilize any line states with just a simple edge termination due to the distinctive topological structure. In fact, the NLSs originally proposed with the theoretical KL model [29] have never been realized, leading to the examination of underlying real-space topology elusive.

In this Letter, we demonstrate an annular (Corbino-disk-shaped) photonic KL for direct observation of the NLSs. Such a Corbino geometry is achieved by warping a KL ribbon into a ring, defining a 2D system confined between two concentric circles, as illustrated in Fig. 1(h). (Similar geometry has recently been used for design of graphene heterostructures and superconducting waveguides [38–40]). In the Corbino-shaped KL, the periodicity is preserved in the azimuthal direction (i.e., the corresponding toroidal direction for the torus geometry). As such, we realize evidently the NLSs as a direct observation of the nontrivial loop states winding along a torus. Furthermore, using a finite-sized KL with open boundaries, we also observe the RBMs and demonstrate their robust propagation and "self-healing" features against perturbation. Through rigorous analysis, we show that the band touching and the NLSs exist in an ideal Corbino-shaped KL of arbitrary size. Our results represent the first realization of nontrivial loop states as direct manifestation of the real-space topological features.

First, we show that a line state cannot be an FB eigenmode in finite KLs regardless of the lattice edge termination, in sharp contrast to the case of Lieb lattices [22]. As depicted in Fig. 1(a), the KL has three lattice sites (A, B, and C) per unit cell, and every lattice site has four nearest neighbors in transverse x-y plane. To excite a particular FB state, a modulated probe beam is sent to propagate through the

lattice along the z direction. Light propagation under paraxial approximation is described by a Schrödingerlike equation [12–19]: $\partial_z\psi(x,y,z) = [(i/2k_0n_0)\nabla_\perp^2 + ik_0\Delta n(x,y)]\psi(x,y,z)$, where $\psi(x,y,z)$ is the envelope of the electric field. The induced refractive-index profile $\Delta n(x,y)$ acts as an effective potential for the light field. k_0 is the wave number, and n_0 is the bulk refractive index. Under the tight-binding approximation, one can use a discrete model to describe the coupling between lattice sites. By Fourier transforming the tight-binding Hamiltonian into k space, one can obtain

$$H_k = 2t\begin{pmatrix} 0 & \cos k_1 & \cos k_2 \\ \cos k_1 & 0 & \cos k_3 \\ \cos k_2 & \cos k_3 & 0 \end{pmatrix}, \tag{1}$$

where t is the hopping amplitude (or coupling constant) for the nearest-neighbor sites. The wave vectors are $k_n = \boldsymbol{k}\cdot\boldsymbol{\alpha}_n$, and α_n is illustrated in Fig. 1(a). Then, we can obtain the eigenvalues of H_k, as the energy spectrum with three bands: $E_{\mathrm{FB}} = -2t, E_\pm(k_x,k_y) = t\{1 \pm [4(\cos^2 k_1 + \cos^2 k_2 + \cos^2 k_3) - 3]^{1/2}\}$. The two dispersive bands ($E_\pm$) intersect at two inequivalent Dirac points like that of the honeycomb lattices [41,42], and the second band touches the bottom FB (E_{FB}) at the center of the first Brillouin zone. In FB lattices, one can always find a set of CLSs as degenerate eigenstates, whose energy is the same no matter where they reside in the lattice. A fundamental CLS (ring mode) [19,43] of the KL is illustrated in Fig. 1(a), where the wave amplitude remains nonzero only at the six lattice sites. Other kinds of CLSs can be constructed by linear superpositions [14,15,18,19]. However, the CLSs cannot span the FB completely because there always exists a vanishing linear combination [29]. The missing states, namely, the NLSs, manifest the topological structure of the lattice in real space. Since a torus geometry is hard to fabricate experimentally, a natural question is whether the line states should exist in a truncated KL under appropriate open boundaries (as for the Lieb lattice [22]). We show below this is not the case due to the fundamental difference of the topological structures of the lattices.

Let us consider the FB model in a photonic KL with open boundaries. The lattice can be terminated into a finite region with four different edges [see Supplemental Material (SM) for details [44]]. As a typical example, we consider only one case here shown in Fig. 1(e), which has in both left and right sides a zigzag-armchair edge. As illustrated in Fig. 1(e), a line state occupies only B and C sublattices, and it can be described by $|\psi_{\mathrm{LS}}\rangle = c_0(|B_1\rangle - |C_1\rangle + |B_2\rangle - |C_2\rangle + |B_3\rangle - |C_3\rangle + |B_4\rangle)$, where c_0 is a normalization constant. Applying the tight-binding Hamiltonian to this line state, we have $H_k|\psi_{\mathrm{LS}}\rangle = c_0 t(-|B_1\rangle + 2|C_1\rangle - 2|B_2\rangle + 2|C_2\rangle - 2|B_3\rangle + 2|C_3\rangle - |B_4\rangle)$, where we have considered only nonvanishing terms, so $\langle\psi_{\mathrm{LS}}|H_k|\psi_{\mathrm{LS}}\rangle$ does not equal to a constant. From this simple calculation, one can see that $|\psi_{\mathrm{LS}}\rangle$ is not an eigenmode of the KL because we obtain different coefficients at two ending sites (B_1 and B_4) compared with the bulk sites (C_1, B_2, C_2, B_3, and C_3). If the periodic BC is assumed, identifying B_1 and B_4, $|\psi_{\mathrm{LS}}\rangle$ can become an eigenmode, which would require delicate design of the boundary passivation as detailed in the SM, Sec. S1 [44].

For the above reason, the line states cannot be stable in the finite KLs, and thus cannot effectively unveil the topological feature of the NLSs under an infinite or periodic FB system. In what follows, we show two alternative ways to observe the NLSs directly in a photonic platform. First, we establish a finite KL with flat-edge termination, equivalent to cutting a torus [Fig. 1(d)] in both toroidal and poloidal directions along the noncontractible loops and unfolding it into a 2D plane. We observe localized loop states along its entire boundary illustrated in Figs. 1(f) and 1(g) as the direct demonstration of the RBMs. Second, we optically "fabricate" a Corbino geometry of the KL discussed above [Fig. 1(h)] to directly observe the NLSs.

Our experiments are based on photonic lattices formed by *continuous-wave (cw)* laser writing of waveguides using the technique established already for the Lieb lattices [22], essentially site-to-site optical induction in a bulk photorefractive nonlinear crystal (SBN, with dimensions $5 \times 10 \times 5$ mm^3). Although the mechanism is quite different, the writing method used here is somewhat similar to femtosecond laser-writing waveguides in glass [45,46]. A laser beam ($\lambda = 532$ nm) is used to illuminate a spatial light modulator (SLM), which controls the amplitude and phase of the writing beam with reconfigurable input positions. After the SLM, a $4F$ system is used to generate a quasinondiffracting zone of the writing beam through the biased crystal. All waveguides remain intact during the writing process. To examine the induced lattice, we illuminate a weak extraordinarily polarized quasi-plane wave to probe the written waveguide array. At the back facet of the crystal, we see that the otherwise uniform probe beam becomes discretely guided into the lattice sites, indicating the desired KL has been established [Fig. 2(a)]. With such a writing technique, photonic KLs with different edge terminations are established, where we found that the line states indeed cannot preserve in finite KLs (see SM [44] for details).

Next, we present our results of the RBMs spanning the whole boundary of the finite lattice, as observing the RBMs is in a sense equivalent to observing the NLSs [30]. Typical experimental and simulation results for the RBMs are presented in Fig. 2. Figs. 2(a1) and 2(a2) show the KL terminated with flat edges, and the lattice spacing is about 34 μm. The RBM1 corresponding to Fig. 1(f) can be considered as a combination of four NLSs by cutting the torus in two orthogonal directions [30]. To observe this boundary mode, an input probe beam is shaped into a parallelogram pattern with its phase modulated by the SLM so that adjacent sites have opposite phase. When such a

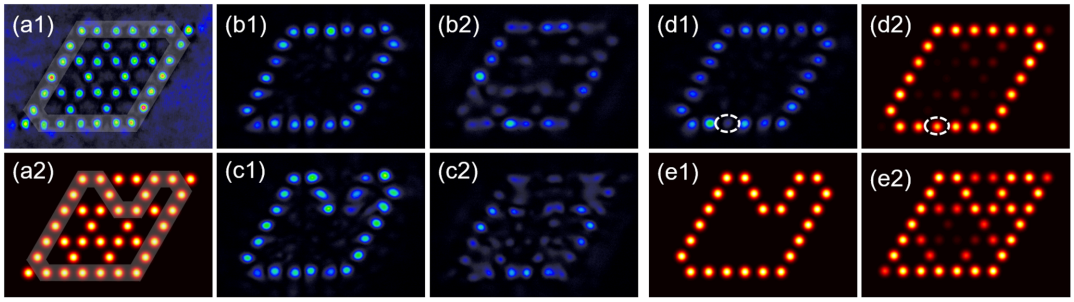

FIG. 2. Realization of RBMs in a finite-sized KL with flat-cutting edges. (a1),(a2) The lattice from (a1) experiment and (a2) simulation, where the shadow in (a1) and (a2) marks the input beam of RBM1 and RBM2, respectively. (b1),(b2) Experimental results of RBM1 under (b1) out-of-phase and (b2) in-phase input conditions, corresponding to Fig. 1(f). (c1),(c2) Experimental results of RBM2, corresponding to Fig. 1(g). (d1),(d2) Excitation of RBM1 with a defect site of imperfect input phase from (d1) experiment and (d2) simulation to 20 cm propagation distance. (e1),(e2) Simulation results corresponding to (c1),(c2).

probe beam is launched into the lattice boundary, it preserves its necklacelike pattern after passing through the lattice [Fig. 2(b1)]. For comparison, the necklace deteriorates if the neighboring sites are in phase [Fig. 2(b2)], as the energy of the boundary mode couples into other sites out of the loop. On the other hand, the RBM2 corresponding to Fig. 1(g) can be regarded as a linear superposition of RBM1 and a fundamental CLS shown in Fig. 1(a), so there are two defect sites with respect to RBM1 but the loop remains unbroken. Clearly, RBM2 can also be retained after propagating through the lattice with the out-of-phase condition [Figs. 2(c1) and 2(e1)], but not with the in-phase condition [Figs. 2(c2) and 2(e2)] due to the nature of the FB eigenstates.

To further show the stability of the RBMs, we intentionally introduce perturbation to the otherwise uniform loop state in both experiment [Fig. 2(d1)] and numerical simulation [Fig. 2(d2)]. In the example shown for the RBM1, a phase perturbation (about 25%) is added to one "pearl" of the necklacelike mode. After propagating through the lattice, the field at the defect site recovers and the RBM1 restores, which can be seen more clearly from the simulation to a longer propagation distance through the lattice [Fig. 2(d2)]. In other words, the RBM can maintain its shape even if there exists slight energy leakage (because of the finite lattice size and limited propagation distance). As such, the RBM exhibits a "self-healing" feature [22]. From the previous study [30], we know the boundary modes cannot be observed by directly probing energy spectra (since the whole band is degenerate), so this stability against perturbation is the main signature of the RBMs that we observe here in real space.

Finally, we present the results obtained with a Corbino-shaped KL. As illustrated in Fig. 3(a), with this lattice geometry, one can realize the NLS along the toroidal direction, akin to an infinite system in one dimension. For the Corbino geometry, the distances between B and C sublattices are equivalent over each ring and increase with the ring diameter (here we use $B_1C_1 = C_1B_2 = 32\ \mu$m); the distances between A and B (C) sublattices are also equal but these distances within and outside the ring are not dependent (here we use $A_1C_1 = A_1B_1 = 41\ \mu$m and $A_4C_1 = A_4B_2 = 32\ \mu$m). We generate such a Corbino-shaped KL with site-by-site laser writing in the nonlinear crystal, and a typical experimentally established lattice is shown in Fig. 3(b). Then, we launch a ring-shaped necklace pattern under out-of-phase condition to excite the NLS depicted in Fig. 3(a). Corresponding experimental results are shown in Fig. 3(c1), where one can clearly see that the necklace beam remains intact after 10 mm of propagation through the lattice, as verified by numerical simulations to even longer propagation [Figs. 3(c2) and 2(c3)]. For comparison, if the input necklace beam does not have the required alternating phase, it is strongly distorted during propagation [Figs. 3(d1)–3(d3)] since such an input cannot evolve into the NLS. The results in Fig. 3(c) represent a direct demonstration of the NLS originally proposed for the infinite system as the nontrivial FB eigenstate arising from real-space topology [29].

Before closing, a few issues merit discussion. The first is about the fundamental difference between the Corbino- and torus-shaped KLs. Note that the torus geometry corresponds to the usual infinite system with periodic BC satisfied in two orthogonal directions, but in the Corbino geometry it is satisfied along only one direction. To this end, we analyzed the band structure of an ideal Corbino disk of arbitrary size in the Supplemental Material [44]. We show that the FB of the Corbino geometry still supports the band crossing corresponding to that in the torus geometry. However, the counting argument for the number of independent CLSs and NLSs arising from the band crossing changes drastically. We show that there are N [$N = 8$ for the illustrated example in Fig. 1(h)] independent CLSs and only one independent NLS in the Corbino geometry, as opposed to the existence of N-1 CLSs and two NLSs in the torus geometry. Thus, in the Corbino geometry, the band crossing point intrinsically yields only one topological NLS (see SM, Sec. II [44] for details).

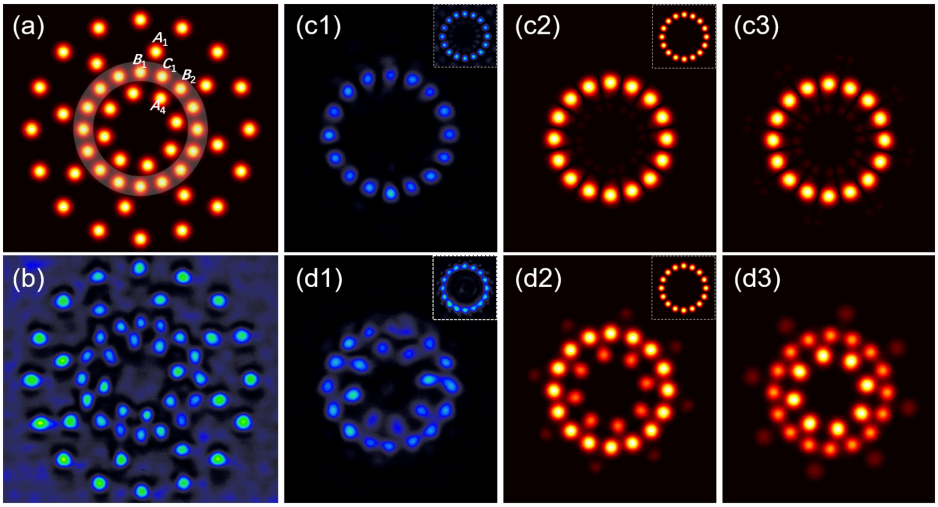

FIG. 3. Direct observation of an NLS in a Corbino-shaped KL. (a) Numerically generated Corbino-shaped KL, where the shadowed circle marks the NLS. (b) Experimentally established lattice corresponding to (a) by site-to-site laser writing. (c1)–(c3) The NLS observed in (c1) experiment and (c2),(c3) simulations at propagation distances of (c2) 1 cm and (c3) 4 cm under out-of-phase condition. (d1)–(d3) Corresponding results under in-phase condition. All insets are taken from the input necklace-shaped probe beam. (For detailed theoretical analysis of the NLS and band touching in the finite Corbino disk, see Supplemental Material, Sec. S2 [44]).

The other issue is about the broader impact of our work based on the KLs. Although kagome and Lieb lattices share some similar properties, being singular FB with band touching protected by discontinuities of their Bloch functions, they do have a fundamental difference: the FB of a Lieb lattice arises due to its bipartite lattice structure, occurs in the middle of its energy spectrum, and gives rise to FB ferrimagnetism when filled with interacting spins [47,48]; the FB of a kagome lattice is based on its line graph structure, lies at an extremum of the single particle spectrum, and hosts FB ferromagnetism [49]. Thus, our finding that finite KLs cannot stabilize the line states but rather the NLSs adds to new understanding of these singular flatbands. On the other hand, in contrast to Lieb lattices, which typically require atom-by-atom construction [24,27], KLs have been readily grown at a large scale. While a major motivation for studying KLs is their exotic spin liquid states [50], recent experiments directly measure the electronic band structure and image the bulk and edge states in KLs [51,52]. Negative FB magnetism has also been demonstrated with a correlated kagome magnet representing a nontrivial flatband system [53]. In photonics, higher-order topological insulators have been realized with the KLs [54,55]. More broadly, the presence of flatbands in various moiré superlattices is believed to be closely connected to the emergence of novel strongly correlated electronic states [56,57]. Thus, our work on topological photonic KLs is of interdisciplinary interest.

In conclusion, we have demonstrated NLSs and RBMs, which are unique topological entities available in the singular FB systems, with a photonic KL platform. We have directly probed the real-space topology of these nontrivial loop states: First, the NLS is observed in the judiciously designed KL of Corbino geometry, where the periodic BC is realized along a closed loop winding around the 2D Corbino disk, just as the NLS winding across a 3D torus; Second, the robustness of the RBM is realized, against the addition of any CLS or defect. Theoretically, we have proved that the band touching is still topologically protected in an ideal Corbino KL. Our direct observation and rigorous analysis of the NLSs indicate that the KLs have a band-crossing singularity in momentum space arising from real-space topology. Our work in a convenient photonic platform may lead to new understanding of some intriguing fundamental phenomena relevant to strongly interacting systems.

We thank Sergej Flach and the referees for insightful comments. This research is supported by the National key R&D Program of China under Grant (No. 2017YFA0303800), NNSF (91750204, 11674180, 11922408, 11704102), PCSIRT (IRT0149) and 111 Project (No. B07013) in China, and Institute for Basic Science in Korea (IBS-R024-Y1, IBS-R009-D1), National Research Foundation of Korea (0426-20170012, 0426-20180011), POSCO Science Fellowship (0426-20180002), and U.S. Army Research Office (W911NF-18-1-0137).

*tanya@nankai.edu.cn
†zgchen@nankai.edu.cn
‡These authors contributed equally to this work.

[1] M. Goda, S. Nishino, and H. Matsuda, Phys. Rev. Lett. **96**, 126401 (2006).
[2] J. T. Chalker, T. S. Pickles, and P. Shukla, Phys. Rev. B **82**, 104209 (2010).

[3] S. D. Huber and E. Altman, Phys. Rev. B **82**, 184502 (2010).
[4] E. Tang, J.-W. Mei, and X.-G. Wen, Phys. Rev. Lett. **106**, 236802 (2011).
[5] T. Neupert, L. Santos, C. Chamon, and C. Mudry, Phys. Rev. Lett. **106**, 236804 (2011).
[6] V. I. Iglovikov, F. Hébert, B. Grémaud, G. G. Batrouni, and R. T. Scalettar, Phys. Rev. B **90**, 094506 (2014).
[7] L. Ge, Phys. Rev. A **92**, 052103 (2015).
[8] M. I. Molina, Phys. Rev. A **92**, 063813 (2015).
[9] S. Peotta and P. Törmä, Nat. Commun. **6**, 8944 (2015).
[10] F. Baboux, L. Ge, T. Jacqmin, M. Biondi, E. Galopin, A. Lemaître, L. Le Gratiet, I. Sagnes, S. Schmidt, H. E. Türeci, A. Amo, and J. Bloch, Phys. Rev. Lett. **116**, 066402 (2016).
[11] A. Julku, S. Peotta, T. I. Vanhala, D. H. Kim, and P. Törmä, Phys. Rev. Lett. **117**, 045303 (2016).
[12] D. Leykam, A. Andreanov, and S. Flach, Adv. Phys. X **3**, 1473052 (2018).
[13] D. Guzmán-Silva, C. Mejía-Cortés, M. A. Bandres, M. C. Rechtsman, S. Weimann, S. Nolte, M. Segev, A. Szameit, and R. A. Vicencio, New J. Phys. **16**, 063061 (2014).
[14] R. A. Vicencio, C. Cantillano, L. Morales-Inostroza, B. Real, C. Mejia-Cortes, S. Weimann, A. Szameit, and M. I. Molina, Phys. Rev. Lett. **114**, 245503 (2015).
[15] S. Mukherjee, A. Spracklen, D. Choudhury, N. Goldman, P. Öhberg, E. Andersson, and R. R. Thomson, Phys. Rev. Lett. **114**, 245504 (2015).
[16] S. Mukherjee and R. R. Thomson, Opt. Lett. **40**, 5443 (2015).
[17] S. Weimann, L. Morales-Inostroza, B. Real, C. Cantillano, A. Szameit, and R. A. Vicencio, Opt. Lett. **41**, 2414 (2016).
[18] S. Xia, Y. Hu, D. Song, Y. Zong, L. Tang, and Z. Chen, Opt. Lett. **41**, 1435 (2016).
[19] Y. Zong, S. Xia, L. Tang, D. Song, Y. Hu, Y. Pei, J. Su, Y. Li, and Z. Chen, Opt. Express **24**, 8877 (2016).
[20] C. Huang, F. Ye, X. Chen, Y. V. Kartashov, V. V. Konotop, and L. Torner, Sci. Rep. **6**, 32546 (2016).
[21] E. Travkin, F. Diebel, and C. Denz, Appl. Phys. Lett. **111**, 011104 (2017).
[22] S. Xia, A. Ramachandran, S. Xia, D. Li, X. Liu, L. Tang, Y. Hu, D. Song, J. Xu, D. Leykam, S. Flach, and Z. Chen, Phys. Rev. Lett. **121**, 263902 (2018).
[23] S. Taie, H. Ozawa, T. Ichinose, T. Nishio, S. Nakajima, and Y. Takahashi, Sci. Adv. **1**, e1500854 (2015).
[24] R. Drost, T. Ojanen, A. Harju, and P. Liljeroth, Nat. Phys. **13**, 668 (2017).
[25] Y. Nakata, T. Okada, T. Nakanishi, and M. Kitano, Phys. Rev. B **85**, 205128 (2012); S. Kajiwara, Y. Urade, Y. Nakata, T. Nakanishi, and M. Kitano, Phys. Rev. B **93**, 075126 (2016).
[26] V. Goblot, B. Rauer, F. Vicentini, A. Le Boité, E. Galopin, A. Lemaître, L. Le Gratiet, A. Harouri, I. Sagnes, S. Ravets, C. Ciuti, A. Amo, and J. Bloch, Phys. Rev. Lett. **123**, 113901 (2019).
[27] M. R. Slot, T. S. Gardenier, P. H. Jacobse, G. C. P. van Miert, S. N. Kempkes, S. J. M. Zevenhuizen, C. M. Smith, D. Vanmaekelbergh, and I. Swart, Nat. Phys. **13**, 672 (2017).
[28] Z. Lin, J.-H. Choi, Q. Zhang, W. Qin, S. Yi, P. Wang, L. Li, Y. Wang, H. Zhang, Z. Sun, L. Wei, S. Zhang, T. Guo, Q. Lu, J.-H. Cho, C. Zeng, and Z. Zhang, Phys. Rev. Lett. **121**, 096401 (2018).
[29] D. L. Bergman, C. Wu, and L. Balents, Phys. Rev. B **78**, 125104 (2008).
[30] J.-W. Rhim and B.-J. Yang, Phys. Rev. B. **99**, 045107 (2019).
[31] B. Moulton, J. Lu, R. Hajndl, S. Hariharan, and M. J. Zaworotko, *Angew. Chem. Int. Ed. Engl.* 41, 2821 (2002).
[32] K. J. H. Law, A. Saxena, P. G. Kevrekidis, and A. R. Bishop, Phys. Rev. A **79**, 053818 (2009).
[33] Q. Chen, S. C. Bae, and S. Granick, Nature (London) **469**, 381 (2011).
[34] G.-B. Jo, J. Guzman, C. K. Thomas, P. Hosur, A. Vishwanath, and D. M. Stamper-Kurn, Phys. Rev. Lett. **108**, 045305 (2012).
[35] M. Nixon, E. Ronen, A. A. Friesem, and N. Davidson, Phys. Rev. Lett. **110**, 184102 (2013).
[36] R. A. Vicencio and C. Mejia-Cortes, J. Opt. **16**, 015706 (2014).
[37] R. Chisnell, J. S. Helton, D. E. Freedman, D. K. Singh, R. I. Bewley, D. G. Nocera, and Y. S. Lee, Phys. Rev. Lett. **115**, 147201 (2015).
[38] M. Kumar, A. Laitinen, and P. Hakonen, Nat. Commun. **9**, 2776 (2018).
[39] Y. Zeng, J. I. A. Li, S. A. Dietrich, O. M. Ghosh, K. Watanabe, T. Taniguchi, J. Hone, and C. R. Dean, Phys. Rev. Lett. **122**, 137701 (2019).
[40] A. J. Kollár, M. Fitzpatrick, and A. A. Houck, Nature (London) **571**, 45 (2019).
[41] O. Peleg, G. Bartal, B. Freedman, O. Manela, M. Segev, and D. N. Christodoulides, Phys. Rev. Lett. **98**, 103901 (2007).
[42] D. Song, V. Paltoglou, S. Liu, Y. Zhu, D. Gallardo, L. Tang, J. Xu, M. Ablowitz, N. K. Efremidis, and Z. Chen, Nat. Commun. **6**, 6272 (2015).
[43] R. A. Vicencio and M. Johansson, Phys. Rev. A **87**, 061803(R) (2013).
[44] See Supplemental Material at http://link.aps.org/supplemental/10.1103/PhysRevLett.124.183901 for the line state existence in finite Kagome lattices and topological protection with Corbino geometry.
[45] K. M. Davis, K. Miura, N. Sugimoto, and K. Hirao, Opt. Lett. **21**, 1729 (1996).
[46] A. Szameit and S. Nolte, J. Phys. B **43**, 163001 (2010).
[47] E. H. Lieb, Phys. Rev. Lett. **62**, 1201 (1989).
[48] H. Wang, S.-L. Yu, and J.-X. Li, Phys. Lett. A **378**, 3360 (2014).
[49] A. Mielke, J. Phys. A **24**, L73 (1991); **25**, 4335 (1992).
[50] H. Takagi, T. Takayama, G. Jackeli, G. Khaliullin, and S. E. Nagler, Nat. Rev. Phys. **1**, 264 (2019).
[51] Z. Li, J. Zhuang, L. Wang, H. Feng, Q. Gao, X. Xu, W. Hao, X. Wang, C. Zhang, K. Wu, S. Dou, L. Chen, Z. Hu, and Yi Du, Sci. Adv. **4**, eaau4511 (2018).
[52] M. Kang *et al.*, Nat. Mater. **19**, 163 (2020).
[53] J.-X. Yin, S. S. Zhang, G. Chang, Q. Wang, S. S. Tsirkin, Z. Guguchia, B. Lian, H. Zhou, K. Jiang, I. Belopolski, N. Shumiya, D. Multer, M. Litskevich, T. A. Cochran, H. Lin, Z. Wang, T. Neupert, S. Jia, H. Lei, and M. Z. Hasan, Nat. Phys. **15**, 443 (2019).
[54] H. Xue, Y. Yang, F. Gao, Y. Chong, and B. Zhang, Nat. Mater. **18**, 108 (2019).

[55] A. El Hassan, F. K. Kunst, A. Moritz, G. Andler, E. J. Bergholtz, and M. Bourennane, Nat. Photonics **13**, 697 (2019).

[56] Y. Cao, V. Fatemi, A. Demir, S. Fang, S. L. Tomarken, J. Y. Luo, J. D. Sanchez-Yamagishi, K. Watanabe, T. Taniguchi, E. Kaxiras, R. C. Ashoori, and P. Jarillo-Herrero, Nature (London) **556**, 80 (2018).

[57] Y. Cao, V. Fatemi, S. Fang, K. Watanabe, T. Taniguchi, E. Kaxiras, and P. Jarillo-Herrero, Nature (London) **556**, 43 (2018).